View metadata, citation and similar papers at core.ac.uk
brought to you by CORE
provided by NASA Technical Reports Server

Rapid Neutron Capture in Supernova Explosions

J.W. Truran* and W.D. Arnett**

Institute for Space Studies
Goddard ~~Space Flight Center,~~ NASA
New York, N.Y.

S. Tsuruta

Smithsonian Astrophysical Observatory
Cambridge, Mass.

and

A.G.W. Cameron

Belfer Graduate School of Science
Yeshiva University
New York, N.Y.

and

Institute for Space Studies
Goddard Space Flight Center, NASA
New York, N.Y.

N67-39075
(ACCESSION NUMBER) (THRU) 1
(PAGES) 34 (CODE)
(NASA CR OR TMX OR AD NUMBER) TMX-60443 (CATEGORY) 29
FACILITY FORM 602

GPO PRICE $
CFSTI PRICE(S) $
Hard copy (HC) $3.00
Microfiche (MF) .65
ff 653 July 65

Abstract

The implications of recent studies of the dynamics of the cores of highly evolved massive stars are considered with regard to the general problems of nucleosynthesis. The typical conditions estimated for these models are shown to be very promising for the process of element synthesis by neutron capture on a fast time scale (the r-process of Burbidge et al, 1957).

---

*Present address: Belfer Graduate School of Science, Yeshiva University, N.Y.

**Present address: Kellogg Radiation Laboratory, California Institute of Technology, Pasadena, California.

10/67

I. Introduction

Studies of the thermonuclear reaction mechanisms believed to be responsible for the production of the heavy elements ($A > 40$) have generally been restricted by the lack of a realistic model of the stellar environment. Investigations of both the slow and rapid neutron capture processes have involved attempts to fit the observed abundance patterns with various choices for the available neutron flux (Seeger *et al*, 1965). Considerations of the formation of nuclei in the iron peak region have generally been concerned with the deviations of the observed abundances from an equilibrium configuration (Burbidge, Burbidge, Fowler and Hoyle, 1957) or with the nuclear transformations which take place under somewhat arbitrarily specified temperature and density conditions (Truran *et al*, 1966). While such studies have established the role of these processes in the synthesis of the heavy elements, they have not provided a complete picture of the sequence of these processes within the general framework of stellar evolution and nucleosynthesis.

Recent studies of the dynamics of the cores of highly-evolved massive stars (Arnett, 1966 and 1967*a*; Colgate and White, 1966) have revealed that for cores of mass $M_c \lesssim 4\ M_{\odot}$, a considerable fraction of the core mass will be ejected. This mass ejection may be identified with supernova explosions. At the extreme temperature and density conditions realized in the core the matter is composed predominantly of neutrons. As the ejected matter expands and cools, these neutrons may be converted to protons, helium and heavier elements. Preliminary estimates indicate that element synthesis may take place readily under these conditions. In this paper we will consider the implications of this model with regard to the problem of the synthesis of the heavy elements by rapid neutron capture. The possible production of heavy elements in the supernova envelope is also discussed. The formation of iron peak elements in the supernova envelope has been considered in another paper (Truran et al, 1967).

The outline of this paper is as follows. In Section II we review in detail the supernova model on which our calculations are based. In Section III the nuclear reaction network employed in these calculations is defined and a brief discussion of the relevant nuclear physics is presented. The results of our studies of the extent of heavy element production are presented in Section IV. In Section V the abundance configurations predicted in equilibrium for our temperature and density conditions are presented. The three processes of element synthesis which are believed to be responsible for the production of the heavy elements are defined in Section VI. In Section VIII, the implications of the supernova conditions for the process of element synthesis by rapid neutron capture are considered in detail. A brief discussion of other possible neutron capture processes is given in Section VIII.

II. Supernova Model

The paths in the density-temperature plane of two representative mass zones of the 2 $M_{\odot}$ supernova core model of Arnett (1967a; see also Arnett and Cameron, 1967) are shown in Figure 1. In this paper we will be concerned with the innermost ejected layers of the core, as represented by the mass zone at 0.9743 $M_\odot$. The initial model evolves along the adiabat AB because hydrodynamic compression has become rapid compared to neutrino energy loss. The evolution of the 0.9743 $M_\odot$ interior mass zone is extremely rapid from B to C. Inadequate sampling of the calculation (once per thousand time cycles) makes our knowledge of the details of the path uncertain here. Evolving from C to D this material encounters the thermal wave due to energy-transporting neutrinos. After heating, the infall of the material is reversed and it begins to expand from D to E. At E it again encounters the neutrino emission surface. The nonadiabatic evolution along EF is in the thin-approximation region for neutrino transport. The heating processes exceed cooling because the core is expanding and therefore decreasing its "optical" depth for neutrinos (antineutrinos); this results in more rapid energy transfer from the core. Along FG the cooling is almost adiabatic because the neutrino flux is attenuated by spherical geometry and the evolution is too fast for the usual pair annihilation neutrino loss rate to be important (although it is included in the calculation). At G the equilibrium for strong interactions transforming ^{4}He to nucleons begins to favor ^{4}He again.

In the calculation shown in Figure 1, the ratio of neutron and proton number densities was of order unity, so that evolution proceeded along GH. This was an oversimplification of the time-dependent equation of state. Electron capture was assumed to occur only on nuclei, and only if the density was more than 10^{11} gm.cm.$^{-3}$. While this assumption does not affect the behavior of the material which forms the nuclear-density central region, and has little effect on the qualitative hydrodynamic behavior of the ejected mass, a more accurate estimate of the neutron to proton ratio is desirable for a discussion of the implications of this model for element synthesis.

In a subsequent consideration of this problem (Arnett and Cameron, 1967) it was found that the weak interactions should freeze out in the early stages of expansion of the ejected material at a temperature of approximately 20 billion degrees and a density of 7×10^9 gm.cm.$^{-3}$: the neutron to proton ratio realized in this freezing process was approximately 8. This ratio was not found to be a sensitive function of the freezing density. For this neutron to proton ratio only a fraction of the mass will be converted to helium; energy considerations suggest that the evolutionary path shown in Figure 1 will be amended in the manner indicated by the dashed line.

The temperature-density history of the stellar material employed in our considerations of nucleosynthesis in this paper are those obtained in the manner described above. While these results are the best estimates available to date, it should be emphasized that a proper coupling of the hydrodynamic equations, the transport equations for weak interactions and compositional changes has not yet been accomplished, and that rotational effects have not been included (see Colgate, 1967 and Arnett, 1967b). Under these circumstances it seems most prudent to consider that a range of adiabats may be involved either in a single supernova or among a group of supernovae.

The temperature-density profiles employed in our calculations are shown in Figure 2. The initial temperature we consider is 10^{10} °K, at which point the weak interactions have frozen out and the formation of helium from neutrons and protons will proceed rapidly. The density curve shown here is that which has been corrected for the neutron rich behavior; this is the low adiabat. For the high adiabat, the density is reduced by a factor of 10. The decrease in temperature and density with time results from the expansion and cooling of the ejected material.

We are interested in the subsequent thermonuclear evolution of the matter ejected on these supernova models. For the temperature and densities of interest here, the time scale for the conversion of neutrons and protons to ^{4}He is considerably less than the hydrodynamic time scale. The critical consideration is whether the buildup toward heavier nuclei will continue, providing seed nuclei for the process of neutron capture on a fast time scale.

III. Nuclear Reaction Network and Reaction Rates

It was shown in a previous paper (Arnett and Cameron 1967) that substantial amounts of ^{12}C are built up in equilibrium with neutrons, protons, and alpha-particles during the expansion of neutron-rich material along the adiabats discussed above. We wish to determine whether a true nuclear statistical equilibrium will be approached and maintained during the expansion. The nuclear reaction pathways along which the approach to equilibrium will take place presumably lie in the region of very neutron-rich heavy nuclei. The approach to nuclear statistical equilibrium has so far been investigated only for pathways which lie close to the ordinary valley of beta stability (Truran, Cameron, and Gilbert 1966). We do not feel that the techniques used to determine the appropriate nuclear reaction cross sections (Truran, Hansen, Cameron, and Gilbert 1966) will give reliable predictions for very neutron-rich nuclei, and hence extensive calculations have not been made with such nuclei.

Instead, we have adopted the point of view that if nuclear statistical equilibrium can be approached by <u>any</u> set of reaction pathways during the expansion along the adiabat, then it should certainly be attained by the <u>fastest</u> pathway. We have been conservative in that we have required that charged-particle addition reactions must involve alpha-particle capture at least up to nuclear charge numbers equivalent to those encountered in nuclear statistical equilibrium. We have chosen a specific pathway lying close to the ordinary valley of beta stability so that the reaction rates should be fairly reliable.

Accordingly, we have defined a simple nuclear reaction network providing suitable nuclear reaction links connecting neutrons, protons and alpha-particles to ^{86}Kr. This network is illustrated in Figure 3. In the light element region we have included the more important reactions linking neutrons, protons and alpha-particles, as indicated in the figure. The rates employed for these reactions were taken from Wagoner, Fowler and Hoyle (1967).

For the heavy elements, we have considered only alpha-particle and neutron capture reactions. Where experimental date is available, these rates are determined as sums over individual resonance contributions;

otherwise, they are calculated theoretically from average nuclear properties (Truran _et al_, 1966a). Specifically, experimental determinations of the reaction rates were employed for the triple-alpha reaction and for the alpha-capture reactions on ^{12}C, ^{16}O, ^{20}Ne, and ^{24}Mg (Truran _et al_, 1966a,b; Reeves 1965; Fowler _et al_ 1967).

Shaw and Clayton (1967) have considered the enhancement of radiative transition rates by inelastic scattering with electrons and ions in stellar matter. They have pointed out that these effects may be important under non-equilibrium conditions in fusion reactions in the cores of supernovae. In our calculations, both carbon and the heavy elements remain in equilibrium with respect to neutrons and alpha-particles down to a temperature of approximately five billion degrees. At this temperature, the density for the low adiabat considered in our calculations is 8.75×10^7 gm.cm.$^{-3}$ and clearly those effects are not important. In general, this process will become important in mass zones characterized both by considerably higher densities and by shorter expansion time scales.

The relaxation of this nuclear reaction network is governed by the equations for the rates of change of the abundances of the various nuclear species. The non-linear equations for the changes in the number densities of the various constituents have been expressed in a backward difference form and solved by matrix inversion.

IV. Production of Seed Nuclei

We have considered the nuclear transmutations which will take place for a range of temperature and density conditions. In Figure 4 are plotted the mass fractions of the more important nuclear constituents as a function of time for the high density profile. The initial neutron to proton ratio is 8. It is evident from the behavior in the early stages that an equilibrium has been rapidly established among neutrons, protons, alpha-particles and ^{12}C. As the temperature decreases, and the alpha-particle capture past ^{12}C becomes more rapid, the abundances of the light elements and ^{12}C decreases while the abundances of intermediate nuclei and ultimately ^{86}Kr are rapidly increasing. At a temperature of approximately 4 billion degrees (approximately $2x10^{-2}$ sec.) the reactions involving the heavy elements freeze out in the sense that the nuclear reaction time scale becomes long compared to the expansion time scale. The final abundance of ^{86}Kr is 20% by mass.

The results of a similar calculation performed for the lower density profile are shown in Figure 5. Here the build-up of ^{12}C is somewhat impeded by the lower density. However, the final ^{86}Kr abundance still approaches 10% by mass.

The effects of varying the total neutron to proton ratio realized in freezing are shown in Figure 6. Here the ratio N/P=3, and the low density adiabat is employed. Generally, the protons will be converted completely to helium, hence a larger fraction of the mass can be converted to heavy elements. The ^{86}Kr abundance realized in this calculation approaches 50% by mass.

For both of the density profiles considered above, an appreciable fraction of the mass was found to be processed to ^{86}Kr. It is of interest to determine more precisely the limiting conditions under which this buildup process will take place. In Figure 7 are shown the results of a similar calculation performed for an order of magnitude higher adiabat:

$$\rho = 7\mathrm{x}10^3 \, T_9^{\,3}$$

(This is a somewhat unrealistic condition with regard to the supernova model discussed previously; further, the neutron to proton ratio employed is rather high for these conditions.) The abundance of heavy elements produced is approximately five percent by mass. Here ^{46}Ca is the most abundant nucleus, as heavy element production is impeded by the low densities.

These results suggest that the breakthrough past ^{12}C to heavy elements can take place readily under these conditions. It is clear, however, that our simple linear chain past carbon does not provide an accurate representation of the flows through the iron peak and beyond. Specifically, for the high neutron concentration in our calculation the major flow might proceed far into the neutron rich regions. In this regard, these calculations should give an upper limit both on the time scale required and on the ratio of neutrons to seed nuclei for rapid neutron capture.

V. Equilibrium Abundances

The final distribution of seed nuclei for the rapid neutron capture process may be estimated on the assumption that the nuclear reactions are sufficiently rapid that a condition of nuclear statistical equilibrium is established (Hoyle, 1946; Tsuruta and Cameron, 1965). The abundance of a nucleus of atomic number Z and mas number A in equilibrium is given by

$$n(A,Z) = w(A,Z) \left(\frac{2\pi\hbar^2}{MkT}\right)^{\frac{3}{2}(A-1)} (A^{3/2}) \frac{n_n^{(A-Z)} n_p^{Z}}{2^A} \exp[Q(A,Z)/kT]$$

where n_p and n_n are the number densities of free protons and neutrons and $Q(A,Z)$ and $w(A,Z)$ are the binding energy and partition function, respectively, of the nucleus (A,Z).

These equations are supplemented, for our conditions, by the equation for the conservation of mass

$$\rho = \sum_k A_k \, n(A_k,Z_k)/N_o$$

and by an equation specifying the total ratio of neutrons to protons

$$N/P = \sum_k (A_k-Z_k) n(A_k,Z_k) / \sum_k Z_k n(A_k,Z_k)$$

Here N_o is Avagadro's number, and the sums are taken over all nuclear constituents including neutrons and protons. If we specify the temperature, the density and the total ratio of neutrons to protons these equations can be readily solved for the equilibrium number densities.

The equilibrium abundances obtained for a temperature of $4x10^9$ ^oK, a density of $4.48x10^7$ gm.cm.$^{-3}$ and a total neutron to proton ratio of eight are shown in Figure 8. These conditions are those predicted by the low adiabat near the point at which the reactions involving the heavy elements have frozen out. The masses employed for nuclei in the neutron rich regions far from the valley of beta stability are those predicted by the exponential mass formula of Cameron and Elkin (1965).

The peak nucleus in equilibrium under these conditions is ^{78}Ni, having 28 protons and 50 neutrons. It is understandable that this nucleus, possessing "magic" numbers of both protons and neutrons, is exceptionally stable. However, at slightly lower temperatures the peak shifts from ^{78}Ni to ^{120}Sr (38 protons and 82 neutrons). This behavior is evident in Figure 9, where the equilibrium abundance distribution for the same adiabat at a temperature $3x10^9$ ^oK is shown. The major abundance peak under these conditions is thus seen to be one neutron closed shell removed from the valley of beta stability.

The equilibrium abundances for the high adiabat at the same freezing temperature are shown in Figure 10. The total ratio of neutrons to protons is again taken to be 8. At the factor of ten lower density considered here, the abundance peak remains in the vicinity of ^{78}Ni for a temperature of $3x10^9$ ^oK. The shifting of the peak to the $N = 82$ neutron shell occurs for $T \sim 2x10^9$ ^oK, well below the temperatures for which any appreciable buildup of heavy elements by charged particle reactions can take place.

The temperature dependences of the abundances of neutrons, protons and alpha particles are shown in Figure 11. The total number density of nuclei with $Z > 2$ (denoted by $\sum_{Z>2} n(A,Z)$) is also included. The solid lines correspond to the high density adiabatic cooling curve and the dashed lines to the low density case. The peak nuclei under different temperature-density conditions are indicated by their respective mass numbers and charge numbers (A_p, Z_p).

The general trends evident in these equilibrium studies may be summarized as follows. A decrease in temperature, for the same adiabatic density dependence, results in a shifting of the abundance peak toward more neutron rich nuclei. The presence of increased abundances of neutron rich nuclei in equilibrium is also favored by higher densities.

VI. Mechanisms for Heavy Element Production

There are three distinct processes of nucleosynthesis which are thought to be responsible for the production of the heavy elements (Burbidge et al, 1957; Cameron, 1957): neutron capture on slow and fast time scales and the process responsible for the production of the by-passed nuclei. The abundance trends of even mass numbers for these processes are shown in Figure 12 (Cameron, 1967).

Neutron capture on a slow time scale (the s-process) is characterized by neutron capture lifetimes which are long compared to typical beta decay lifetimes in the vicinity of the valley of beta stability; the path of this process therefore proceeds along the valley of beta stability, the abundance distribution peaking at the neutron closed shell positions where the neutron capture cross sections decrease. These are evident in Figure 12 near mass number A = 90, 138 and 208.

If the neutron capture lifetimes are short compared to the appropriate beta decay lifetimes, the neutron capture path will lie far out on the neutron rich side of the valley of beta stability. Such a situation might be realized in the presence of an extreme neutron flux; the temperature must be sufficiently low that progress along the neutron capture chains is not impeded by photodisintegrations. Following the exhaustion of the neutron flux, the capture products approach the valley of beta stability by a series of beta decays. This sequence corresponds to neutron capture on a fast time scale (the r-process).

The abundance features near mass numbers $A \sim 130$ and 195 are generally attributed to this rapid neutron capture process (Seeger et al, 1965).

The bypassed nuclei are nuclei on the neutron deficient side of the valley of beta stability which cannot be produced by any neutron capture process. In principle, these can result from neutron photodisintegration processes or proton capture processes (the p-process) proceeding on the products of earlier neutron capture synthesis. The apparent constancy of the ratio of the abundance level of bypassed nuclei to that for the neutron capture products, evident in Figure 12, is consistent with this picture.

In the subsequent discussion we will be concerned primarily with the conditions under which the production of heavy elements by rapid neutron capture can take place.

VII. Rapid Neutron Capture

We are now prepared to consider the implications of the supernova shock conditions with regard to the problem of element synthesis by rapid neutron capture. We have found that the production of elements in the vicinity of the iron peak and beyond can take place in the early stages of expansion of the ejected material via charged-particle and neutron capture reactions. The charged particle reaction rates decrease rapidly with temperature and a stable abundance configuration is realized at a temperature in the vicinity of 4×10^9 °K. This abundance pattern has been distorted severely by the limited nuclear reaction network we employed; the abundances predicted in equilibrium for the "freezing" conditions should provide a more realistic estimate of those realized in the expanding material.

While the charged-particle reactions are no longer contributing to the buildup of heavy elements below 4×10^9 °K, and progress toward elements of higher Z is impeded, neutron capture buildup under these conditions should be limited only by neutron photodisintegration reactions. The equilibrium calculation displayed in Figure 10 predicts a neutron number density of 1.88×10^{30} cm.$^{-3}$ and a ratio of neutrons to heavy nuclei of approximately 200. As the temperature is further decreased, the neutron photodisintegration rates will decrease, allowing successive neutron captures to proceed toward nuclei which are increasingly beta-unstable.

Seeger et al (1965) have pointed out that if the abundance peaks at A = 130 and 195 are to be understood in terms of nuclear shell structure, an environment characterized by a high temperature and neutron number density ($T \simeq 10^9$ °K, $n_n \simeq 10^{24}$ cm.$^{-3}$) is required. These conditions are necessary, on their model, for the establishment of a thermal equilibrium between the isotopes of any element, neutrons and photons on a time scale which is short compared to typical beta-decay lifetimes. It is clear, however, that these conditions are extremely sensitive to mass formula predictions of the neutron binding energies and beta-decay energies of the neutron rich isotopes formed in the rapid neutron capture process.

We feel that the rapid neutron capture buildup will be terminated either by the exhaustion of the neutron flux or by the expansion of the medium to extremely low densities. In order to determine which of these is the limiting consideration, and to calculate the final abundances resulting from this neutron capture process, the subsequent history of the medium must be followed in detail. This will involve coupling the hydrodynamic equations with the equations governing the nuclear transformations. Two of us (W.D. Arnett and J.W. Truran) are currently involved in the formulation of this problem.

Taken at face value, the conditions we have considered here lead to the formation of a large amount of heavy elements. It also seems likely that many of the elements present in nature in the silicon to iron region have been made in supernova explosions (Truran et al, 1967). The products of the rapid neutron capture process have an observed abundance relative to the silicon to iron region in the range 10^{-4} to 10^{-6}. It is clear, therefore, that of all the mass processed in supernova explosions only a small part can be processed in the manner outlined in this paper. The trends in current supernova models are consistent with this conclusion.

VIII. Other Neutron Capture Processes

There are several features of the observed abundance distribution of the heavy elements which are difficult to account for on the basis of the rapid neutron capture process outlined above; specifically the abundance peak in the vicinity of mass number $A \sim 103$ and that in the rare earth region (see Figure 12). We believe these may have resulted from the exposure of a region containing a few percent by mass of the products of slow neutron capture to a somewhat smaller neutron flux. This condition may be realized in the supernova envelope in the vicinity of the helium burning shell source, during the passage of the shock wave (Truran et al, 1967). We have found that neutrons released in (α,n) reactions proceeding on ^{25}Mg, ^{26}Mg and ^{29}Si resulted in a neutron number density exceeding $2x10^{18}$ particles/cm.^{3} on a time scale of the order of 10^{-2} seconds. In this case the maximum shock temperature must lie close to $3x10^9$ ^oK, sufficient to produce rapid (α,n) reactions but not sufficient to destroy the heavy nuclei by photodisintegration. Detailed calculations of the buildup of the anomalous fast capture peaks resulting from neutron capture on nuclei in the preceding slow neutron capture peaks near A = 90 and 140 have been found to be extremely sensitive to our estimates of the neutron capture cross sections. We are currently undertaking a reevaluation of these cross section calculations. Also, the neutron number density estimated for this model is somewhat low.

Schwarzschild and Harm (1967) have recently carried numerical calculations through the first four million years of shell helium burning for a Population II star of 1.2 solar masses. The thermal instability associated with this shell burning phase results in "relaxation oscillations" in which the main helium shell flash leads to the formation of a convective zone proceeding outward from the shell. When, after nine such cycles, the convective zone reaches the hydrogen-rich layers above, the mixing of protons with the products of helium burning can proceed.

Sanders (1967) has considered the implications of this behavior with regard to s-process nucleosynthesis. He finds that for relatively small admixtures of protons into a carbon (oxygen) region, the major product will be $^{13}C(^{17}O)$. For both of these cases (α,n) reactions proceeding on a somewhat longer time scale may release sufficient neutrons to drive the slow neutron capture process.

These conditions are promising as well with regard to the formation of the anomalous abundance peaks discussed above. The mixing of protons into a carbon and oxygen region will result in the production of ^{14}N as well as ^{13}C and ^{17}O; in fact, for large proton admixtures the ^{14}N abundance will exceed those of ^{13}C and ^{17}O. In the presence of an appreciable helium abundance, this ^{14}N may be destroyed by

$$^{14}N(\alpha,\gamma)^{18}F(\beta^{+}\nu)^{18}O(\alpha,\gamma)^{22}Ne$$

The subsequent passage of a shock wave through such a region may result in the production of a substantial neutron flux by

$$^{22}Ne(\alpha,n)^{25}Mg(\alpha,n)^{28}Si$$

These neutrons would be produced in a region in which slow neutron capture may previously have taken place, providing seed nuclei. We are currently undertaking a study of this process.

Acknowledgements

This work has been supported in part by the U.S. Atomic Energy Commission, the National Aeronautics and Space Administration, and the National Science Foundation. Two of us (J.W.Truran and W.D. Arnett) have held National Academy of Sciences-National Research Council Postdoctoral Resident Research Associateships; we wish to thank Dr. Robert Jastrow for the hospitality of the Goddard Institute for Space Studies. One of us (S. Tsuruta) wishes to thank Mr. Takagi for his assistance with the calculations.

Bibliography

Arnett, W.D. 1966. Can. J. Phys. 44, 2553.

Arnett, W.D. 1967a. Can. J. Phys. 45, 1621.

__________ 1967b. On Supernova Hydrodynamics, preprint.

Arnett, W.D. and Cameron, A.G.W. 1967. Supernova Hydrodynamics and Nucleosynthesis, Can. J. Phys., in press.

Burbidge, E.M., Burbidge, G.R., Fowler, W.A. and Hoyle, F. 1957. Rev. Mod. Phys. 29, 547.

Cameron, A.G.W. 1957. Chalk River Report CRL-41.

Cameron, A.G.W. and Elkin, R.M. 1965. Can. J. Phys. 43, 1288.

Cameron, A.G.W. 1967. A New Table of Abundances of the Elements in the Solar System, preprint.

Colgate, S.A. 1967. Mass Ejection From Supernova, preprint.

Colgate, S.A. and White, R.H. 1966. Astrophys. J. 143, 626.

Fowler, W.A., Caughlan, G.R. and Zimmerman, B.A. 1967. Thermonuclear Reaction Rates, preprint.

Hansen, C.J. 1966. Thesis, Yale University.

Hoyle, F. 1946. Monthly Notices Roy. Astron. Soc. 106, 343.

Reeves, H. 1965. Stellar Energy Sources, Chap. 2 in Stars and Stellar Systems, edited by L.H. Aller and D.B. McLaughlin (University of Chicago Press).

Sanders, R.H. 1967. S-Process Nucleosynthesis in Thermal Relaxation Cycles, preprint.

Schwarzschild, M. and Harm, R. 1967. Hydrogen Mixing by Helium Shell Flashes, preprint.

Seeger, P.A., Fowler, W.A. and Clayton, D.C. 1965. Astrophys. J. Suppl. XI, No. 97.

Shaw, P.B. and Clayton, D.D. 1967. Particle-Induced Electromagnetic De-excitation of Nuclei in Stellar Matter, preprint.

Truran, J.W., Hansen, C.J., Cameron, A.G.W. and Gilbert, A. 1966a. Can. J. Phys. **44**, 151.

Truran, J.W., Cameron, A.G.W. and Gilbert, A. 1966b. Can. J. Phys. **44**, 563.

Truran, J.W., Arnett, W.D. and Cameron, A.G.W. 1967. Can. J. Phys. **45**, 2315.

Tsuruta, S. and Cameron, A.G.W. 1965. Can. J. Phys. **43**, 2056.

Wagoner, R.V., Fowler, W.A. and Hoyle, F. 1967. Astrophys. J., in press.

Figure Captions

Figure 1. Evolution in the density-temperature plane of selected representative mass zones expelled by the 2 $M_\odot$ model of the core of a massive star. Details of the calculation are given in Arnett (1967a). Radiation pressure dominates above the line so designated, and electron degeneracy pressure dominates below the line so designated.

Figure 2. The temperature and density profile employed in our network calculations. This density curve corresponds to the low adiabat; for the high adiabat, the density is reduced by a factor of ten.

Figure 3. Schematic of the nuclear reaction network employed in these calculations. The reactions involving the light nuclei are indicated. Above ^{12}C, a linear chain through ^{62}Ni is defined by (n,γ) and (α,γ) reaction links.

Figure 4. The evolution of a region composed initially of neutrons and protons in the ratio N/P = 8 is shown for the low adiabatic cooling curve. The mass fractions of the more abundant constituents are plotted as a function of time.

Figure 5. The evolution of a region composed initially of neutrons and protons in the ratio N/P = 8 is shown for the high adiabatic cooling curve. The mass fractions of the more abundant constituents are plotted as a function of time.

Figure 6. The evolution of a region composed initially of neutrons and protons in the ratio N/P = 3 is shown for the high adiabatic cooling curve. The mass fractions of the more abundant constituents are plotted as a function of time.

Figure 7. The evolution of a region composed initially of neutrons and protons in the ratio N/P = 8 is shown for the high adiabatic cooling curve: $\rho = 7\times10^3 T_9^3$. The mass fractions of the more abundant constituents are plotted as a function of time.

Figure 8. The equilibrium abundances of nuclei at the freezing temperature ($T = 4\times10^9$ °K) are shown as a function of mass number for the high density adiabatic cooling curve.

Figure 9. The equilibrium abundances of nuclei at a temperature $T = 3\times10^9$ °K for the high density adiabatic cooling curve are shown as a function of mass number.

Figure 10. The equilibrium abundances of nuclei at the freezing temperature ($T = 4\times10^9$ °K) are shown as a function of mass number for the low density adiabatic cooling curve.

Figure 11. The number densities of neutrons, protons and alpha particles and the total number density of heavy elements ($A > 4$) are plotted as a function of temperature for the two adiabats considered.

Figure 12. Trends among heavy nuclei of abundances attributable to neutron capture on fast and slow time scales and to bypassed processes.

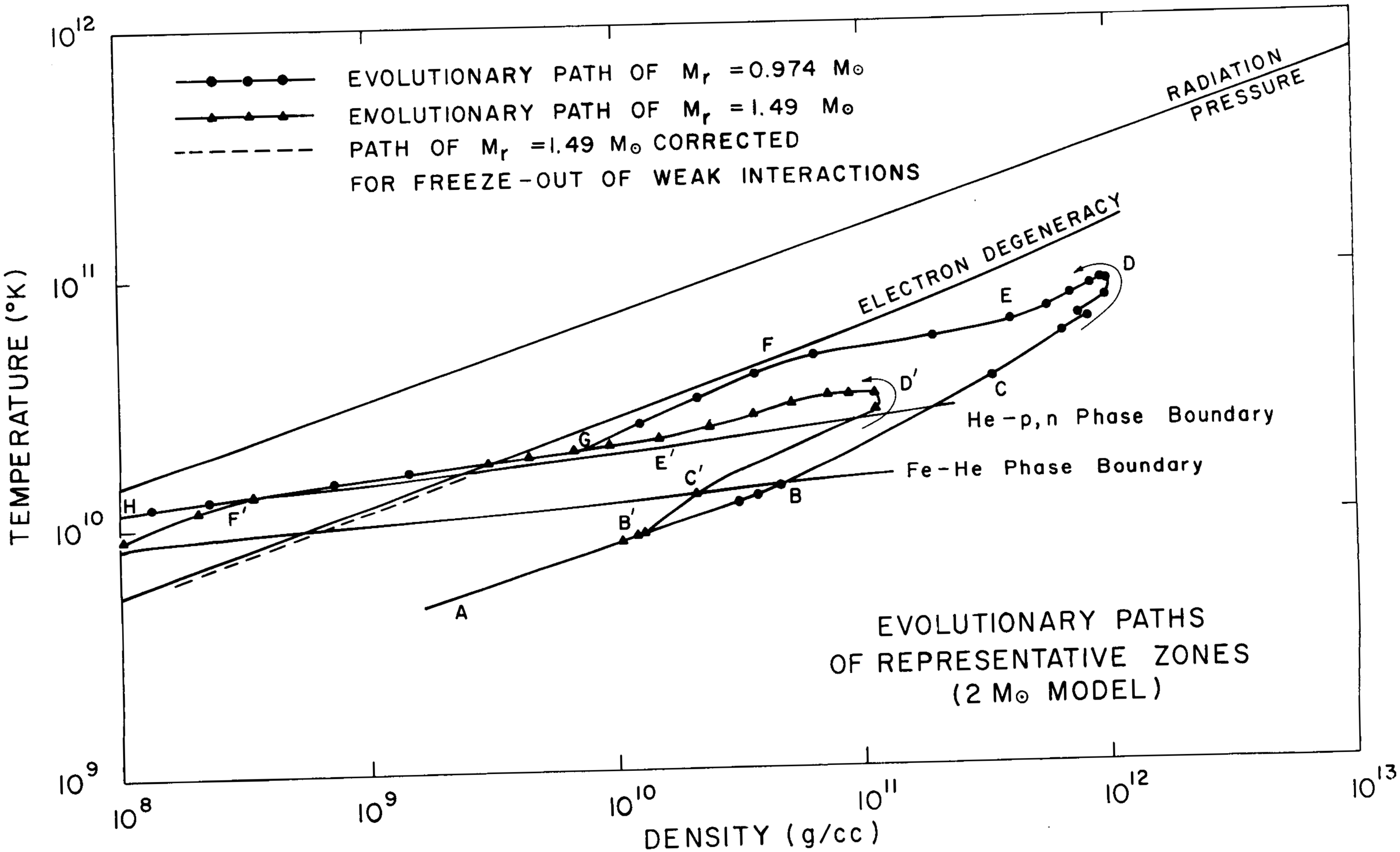

EVOLUTIONARY PATHS OF REPRESENTATIVE ZONES (2 $M_\odot$ MODEL)

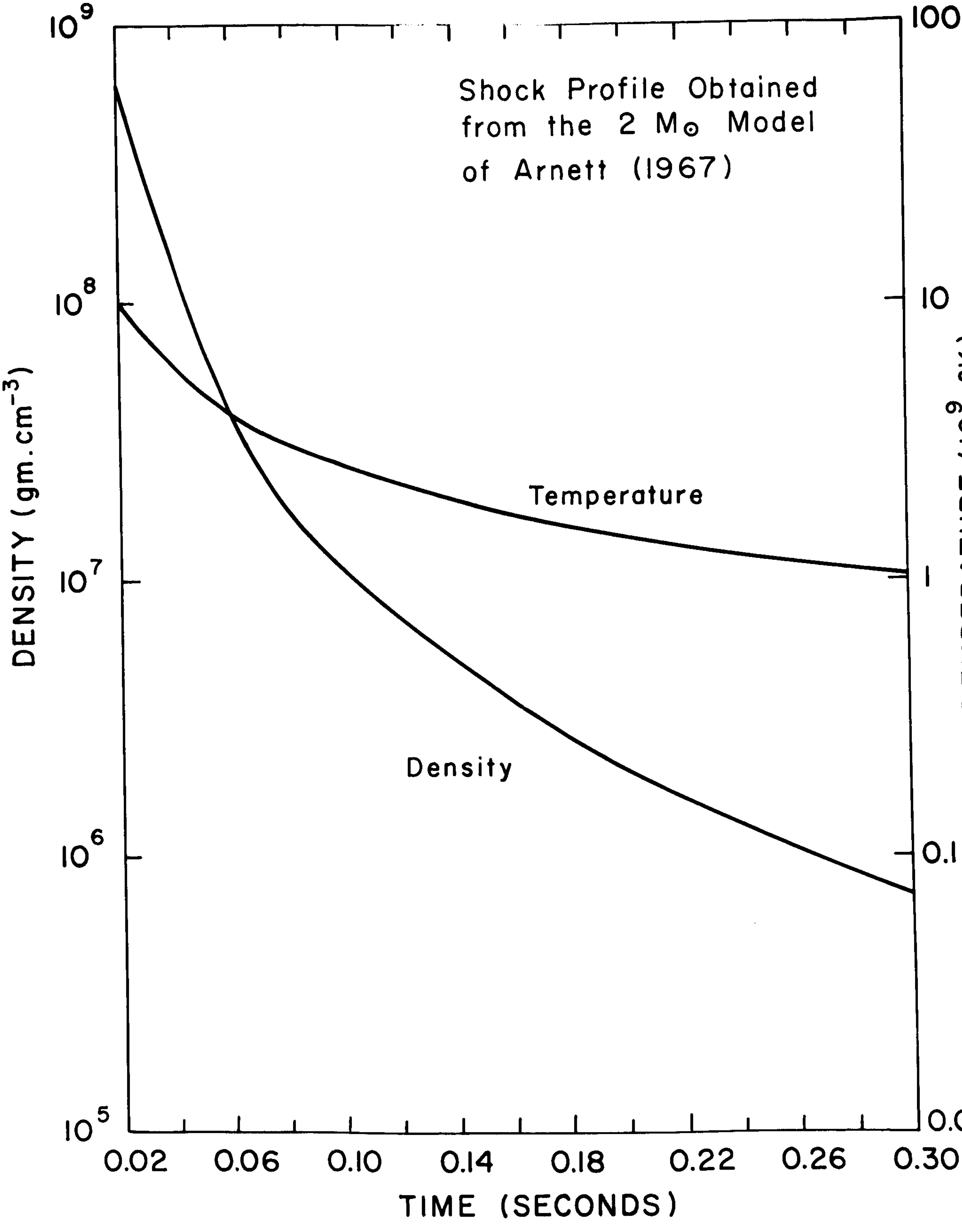
Shock Profile Obtained
from the 2 M⊙ Model
of Arnett (1967)
Temperature
Density
DENSITY (gm.cm⁻³)
TEMPERATURE (10⁹ °K)
TIME (SECONDS)
10⁹
10⁸
10⁷
10⁶
10⁵
100
10
1
0.1
0.01
0.02
0.06
0.10
0.14
0.18
0.22
0.26
0.30

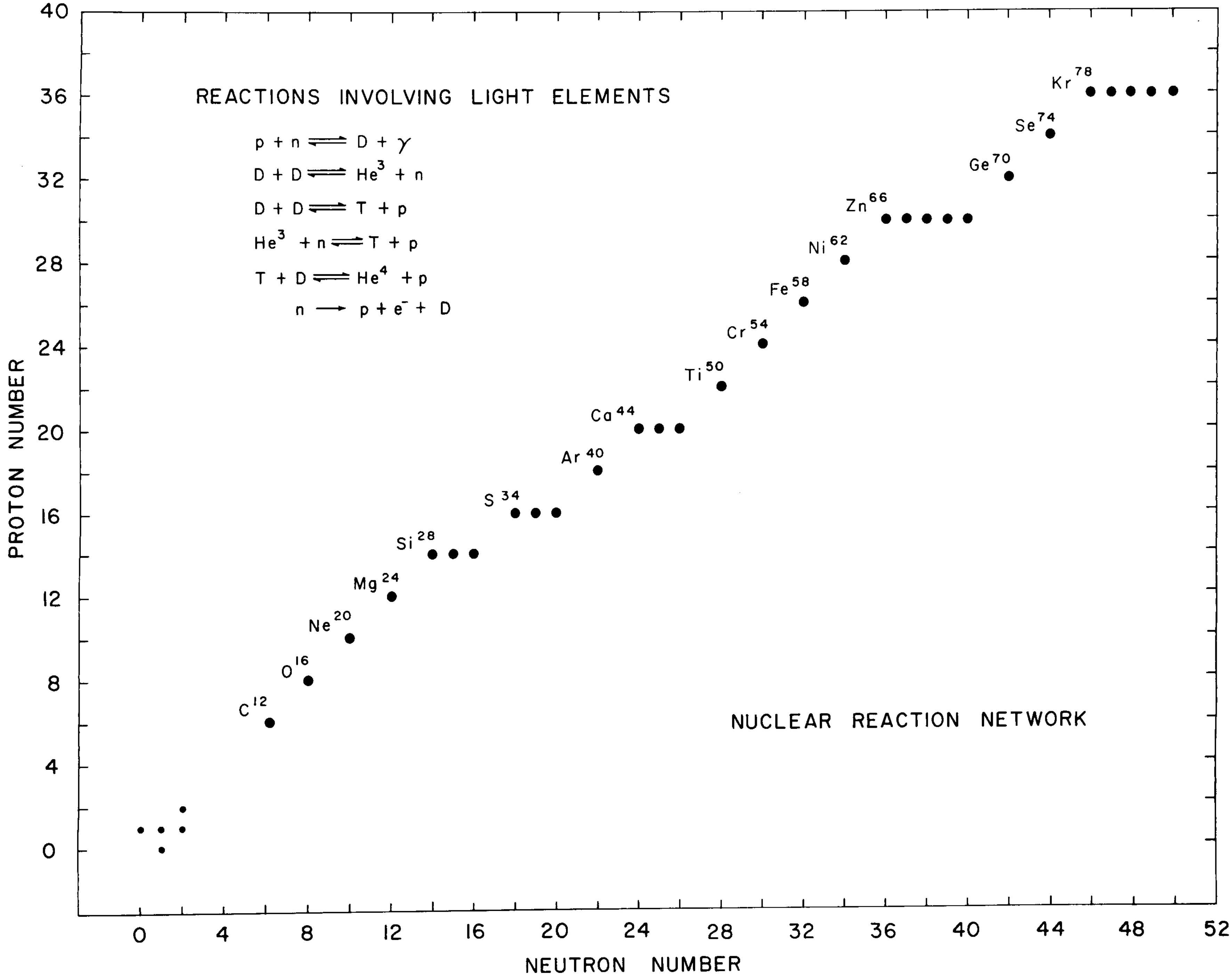

REACTIONS INVOLVING LIGHT ELEMENTS
p + n ⇌ D + γ
D + D ⇌ He3 + n
D + D ⇌ T + p
He3 + n ⇌ T + p
T + D ⇌ He4 + p
n ⟶ p + e- + D
NUCLEAR REACTION NETWORK
PROTON NUMBER
NEUTRON NUMBER
C12
O16
Ne20
Mg24
Si28
S34
Ar40
Ca44
Ti50
Cr54
Fe58
Ni62
Zn66
Ge70
Se74
Kr78

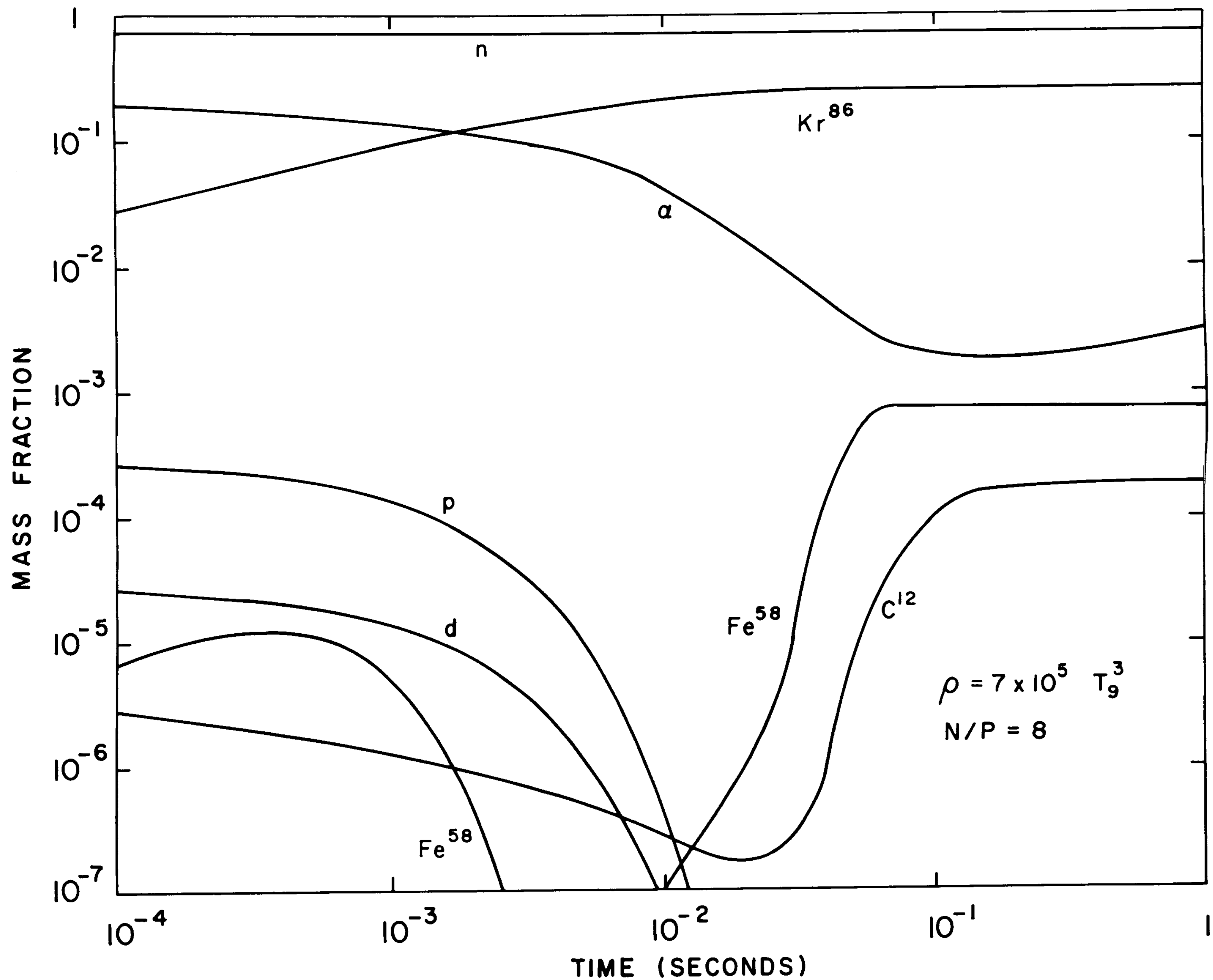

MASS FRACTION
1
10^-1
10^-2
10^-3
10^-4
10^-5
10^-6
10^-7
10^-4
10^-3
10^-2
10^-1
1
TIME (SECONDS)
n
Kr^86
α
p
d
Fe^58
Fe^58
C^12
ρ = 7 x 10^5 T_9^3
N/P = 8

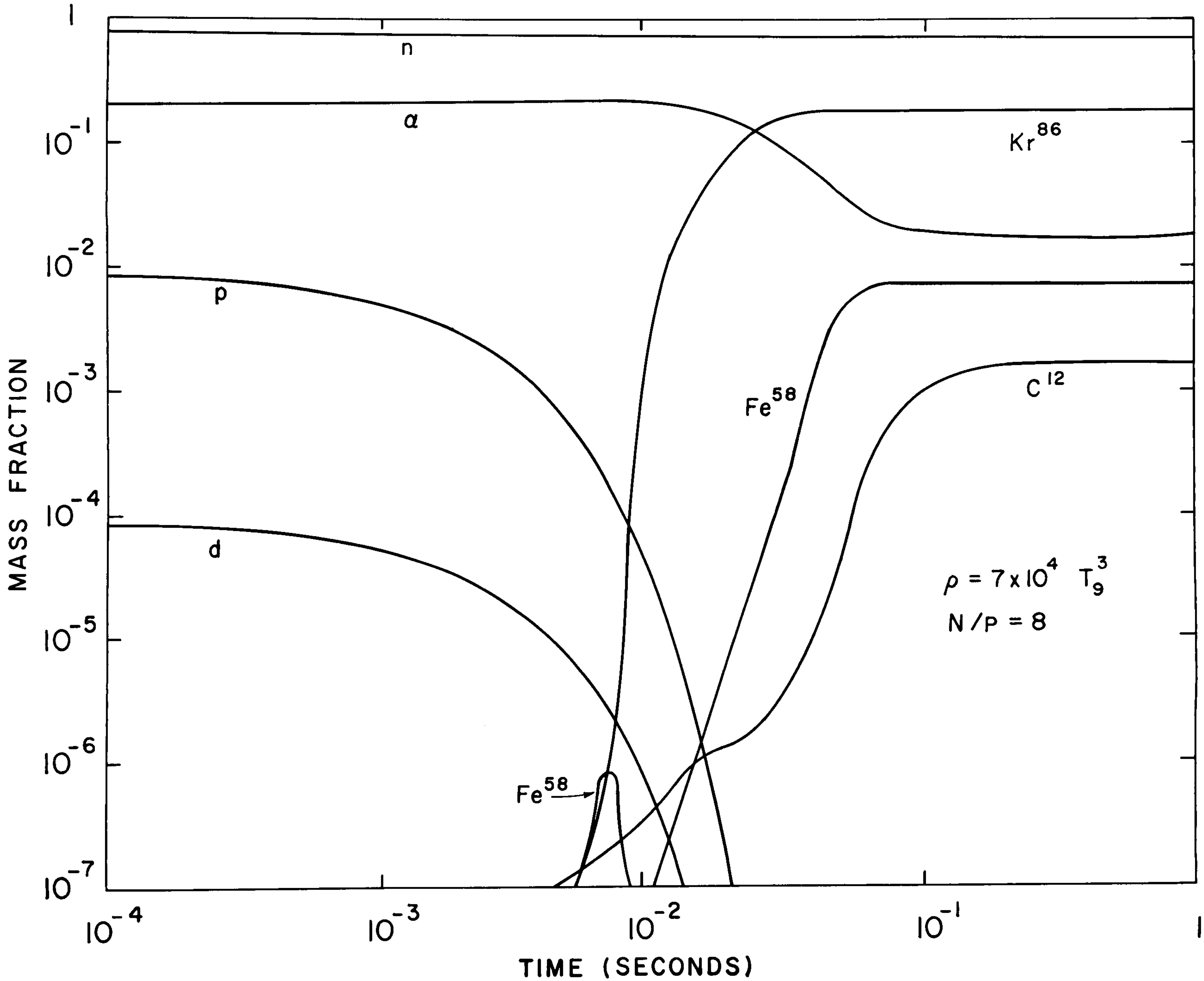

MASS FRACTION
1
10^-1
10^-2
10^-3
10^-4
10^-5
10^-6
10^-7
n
α
p
d
Kr^86
Fe^58
C^12
Fe^58
ρ = 7 x 10^4 T_9^3
N/P = 8
10^-4
10^-3
10^-2
10^-1
1
TIME (SECONDS)

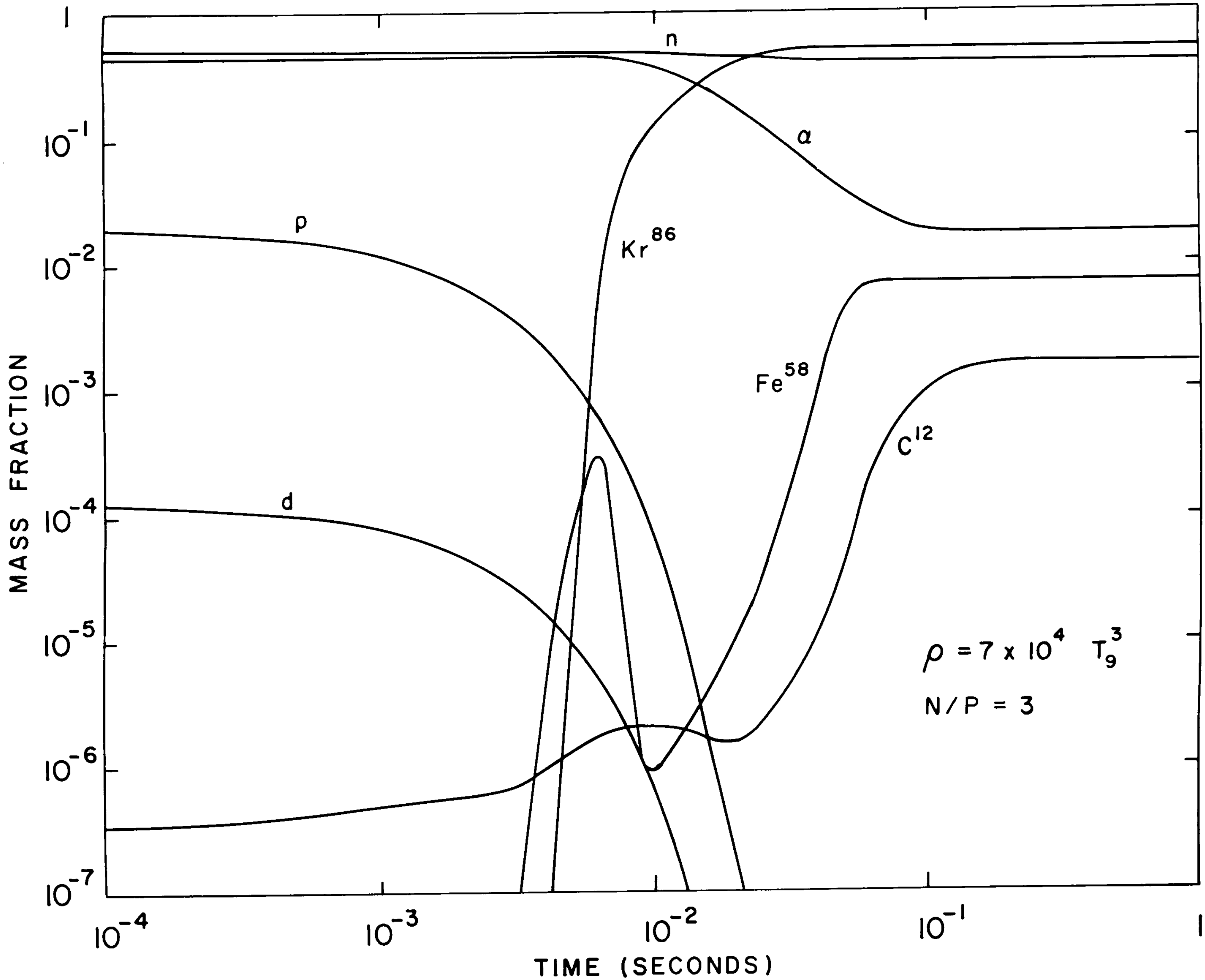

MASS FRACTION
TIME (SECONDS)
1
10-1
10-2
10-3
10-4
10-5
10-6
10-7
10-4
10-3
10-2
10-1
1
n
α
p
d
Kr86
Fe58
C12
ρ = 7 x 104 T93
N/P = 3

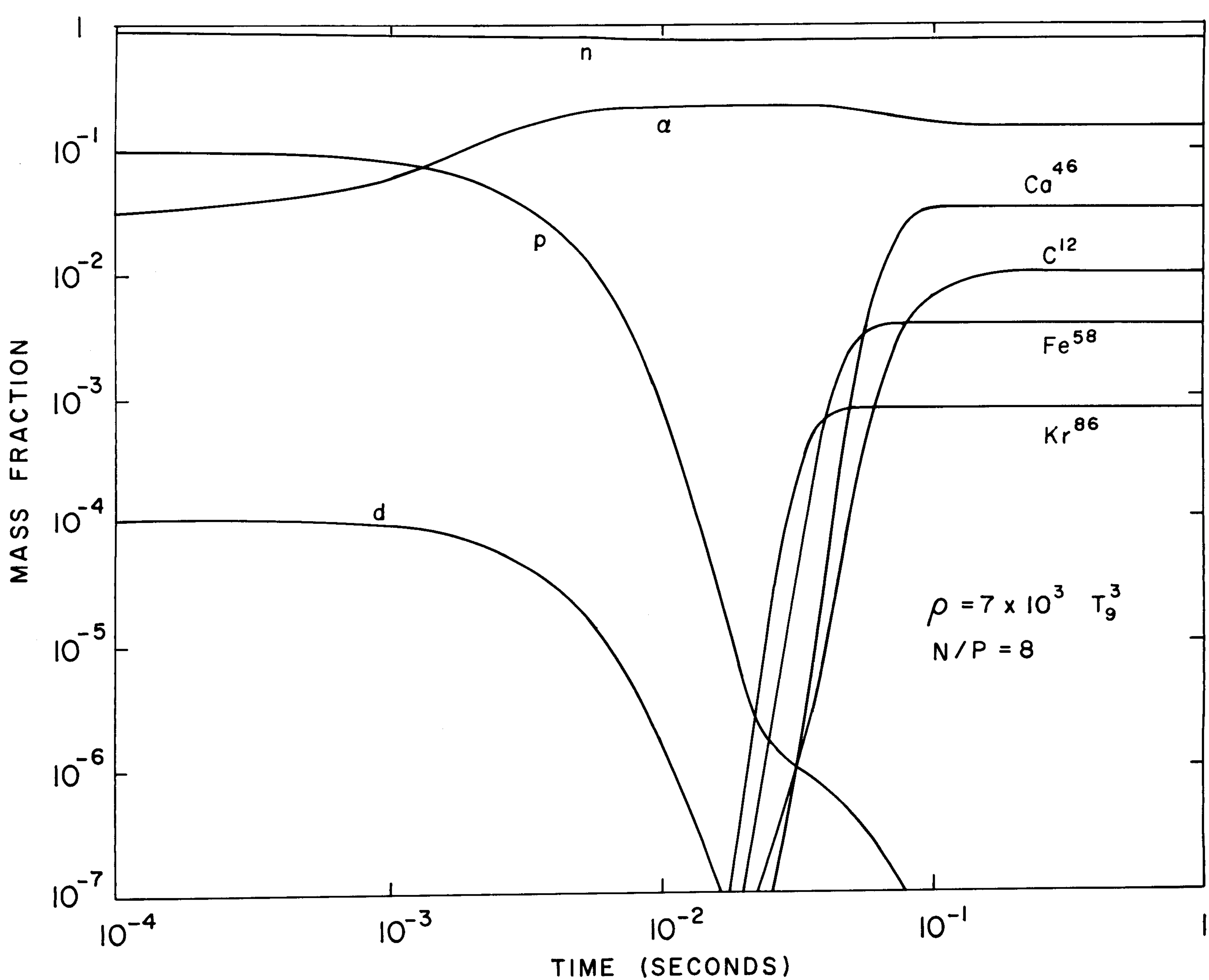

MASS FRACTION
1
10^{-1}
10^{-2}
10^{-3}
10^{-4}
10^{-5}
10^{-6}
10^{-7}
n
α
p
d
Ca^{46}
C^{12}
Fe^{58}
Kr^{86}
$\rho = 7 \times 10^{3}\ T_9^3$
N / P = 8
10^{-4}
10^{-3}
10^{-2}
10^{-1}
1
TIME (SECONDS)

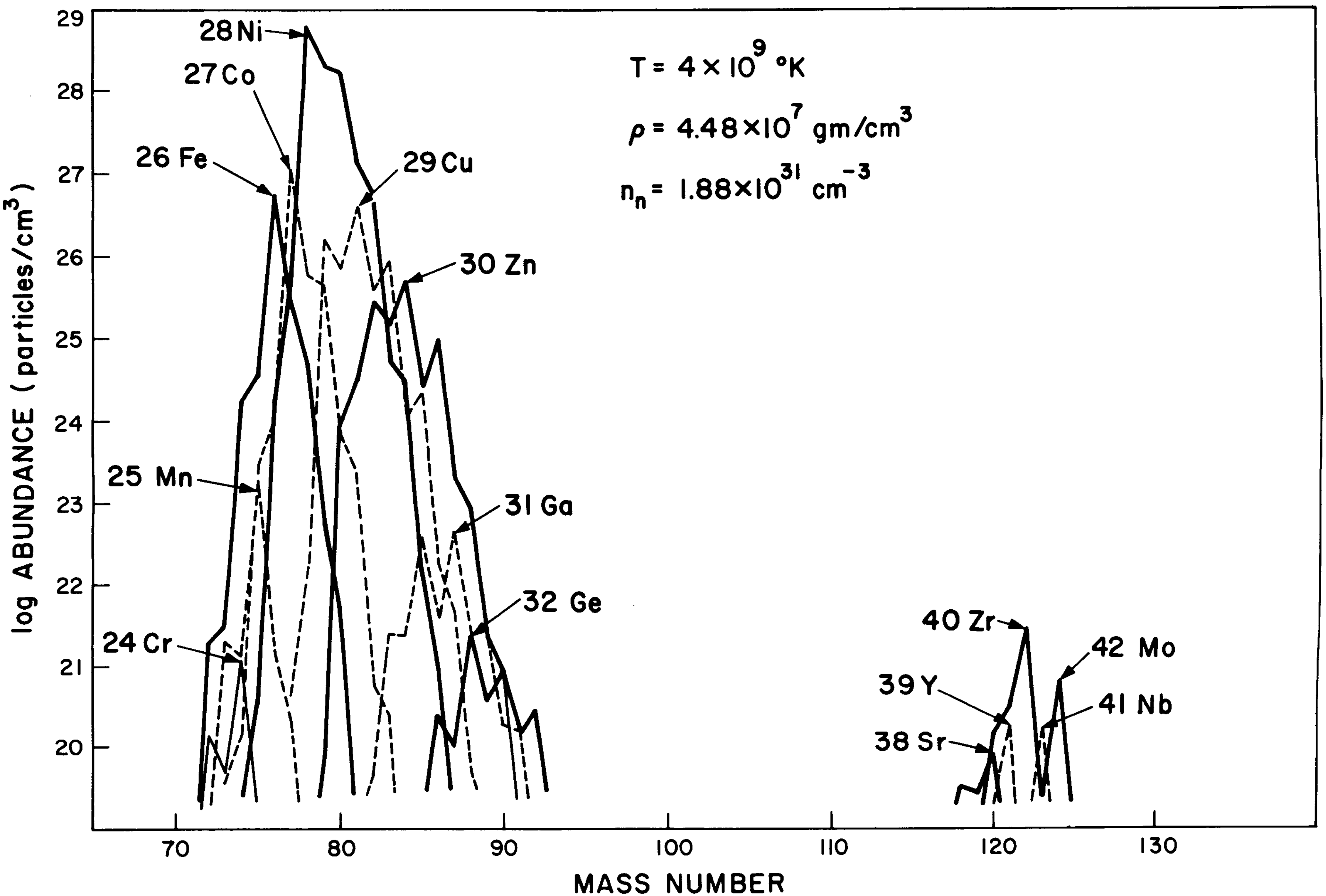
log ABUNDANCE (particles/cm^3)
29
28
27
26
25
24
23
22
21
20
70
80
90
100
110
120
130
MASS NUMBER
28 Ni
27 Co
26 Fe
25 Mn
24 Cr
29 Cu
30 Zn
31 Ga
32 Ge
40 Zr
39 Y
38 Sr
42 Mo
41 Nb
$T = 4 \times 10^9$ °K
$\rho = 4.48 \times 10^7$ gm/cm^3
$n_n = 1.88 \times 10^{31}$ cm^{-3}

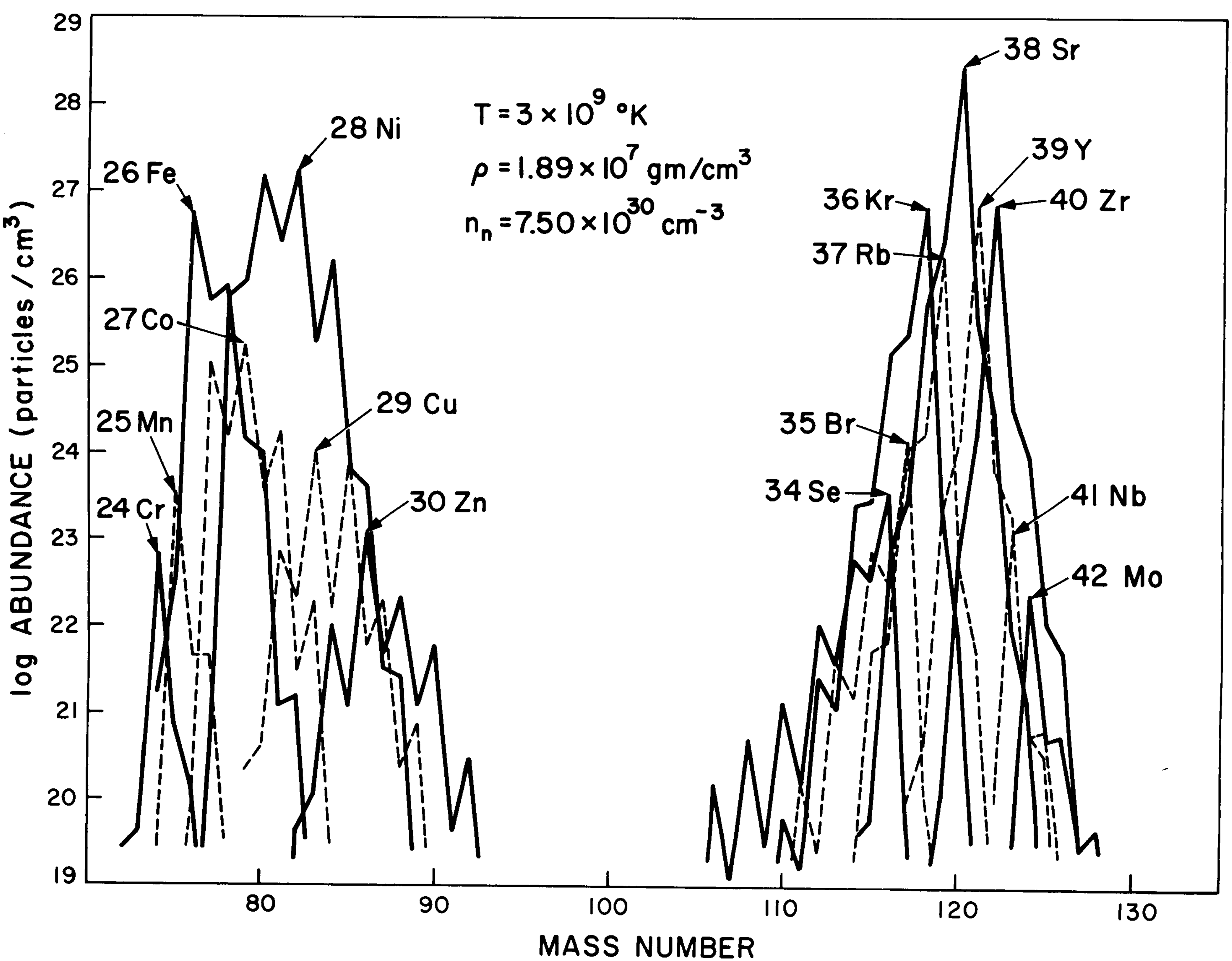
log ABUNDANCE (particles / cm³)
MASS NUMBER
T = 3 × 10⁹ °K
ρ = 1.89 × 10⁷ gm/cm³
n_n = 7.50 × 10³⁰ cm⁻³
24 Cr
25 Mn
26 Fe
27 Co
28 Ni
29 Cu
30 Zn
34 Se
35 Br
36 Kr
37 Rb
38 Sr
39 Y
40 Zr
41 Nb
42 Mo

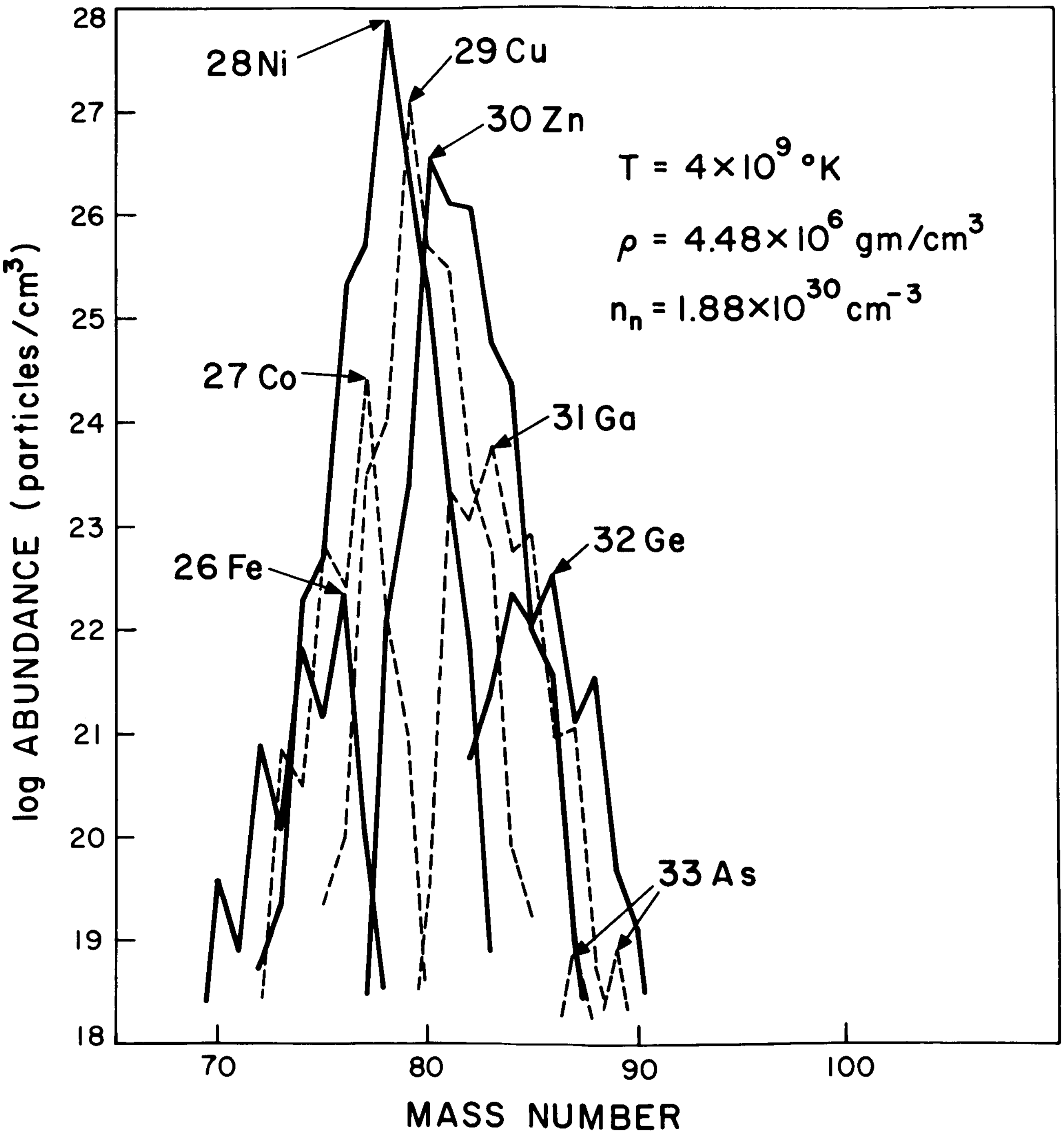
28 Ni
29 Cu
30 Zn
27 Co
31 Ga
26 Fe
32 Ge
33 As
T = 4×10⁹ °K
ρ = 4.48×10⁶ gm/cm³
n_n = 1.88×10³⁰ cm⁻³
log ABUNDANCE (particles/cm³)
MASS NUMBER
28
27
26
25
24
23
22
21
20
19
18
70
80
90
100

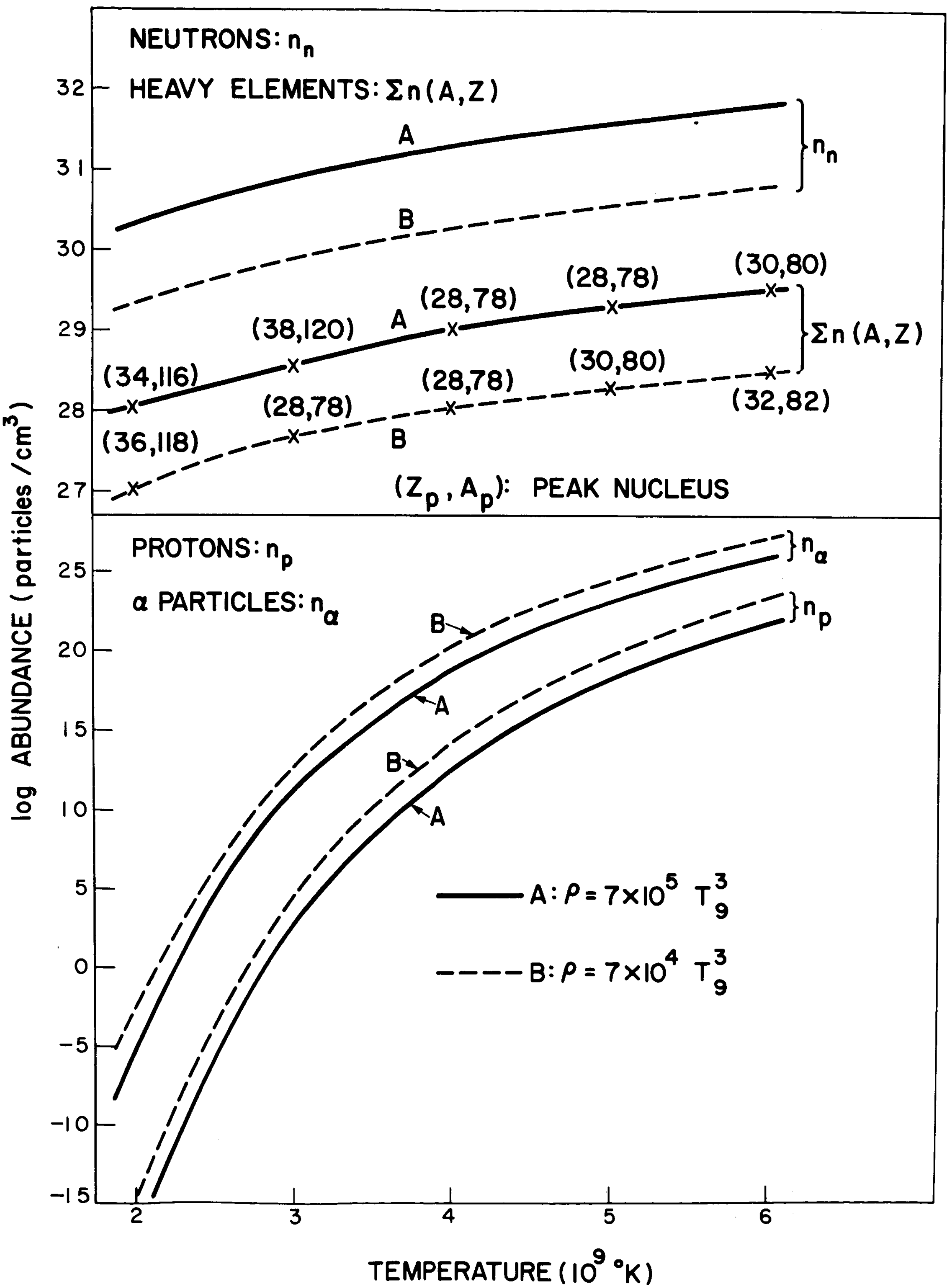

NEUTRONS: n_n
HEAVY ELEMENTS: $\Sigma n(A,Z)$
A
B
n_n
(30,80)
(28,78)
(28,78)
(38,120)
(34,116)
(30,80)
(28,78)
(28,78)
(36,118)
(32,82)
$\Sigma n(A,Z)$
(Z_p, A_p): PEAK NUCLEUS
PROTONS: n_p
α PARTICLES: n_α
n_α
n_p
A: $\rho = 7\times10^5\ T_9^3$
B: $\rho = 7\times10^4\ T_9^3$
log ABUNDANCE (particles /cm^3)
TEMPERATURE (10^9 °K)
32
31
30
29
28
27
25
20
15
10
5
0
−5
−10
−15
2
3
4
5
6

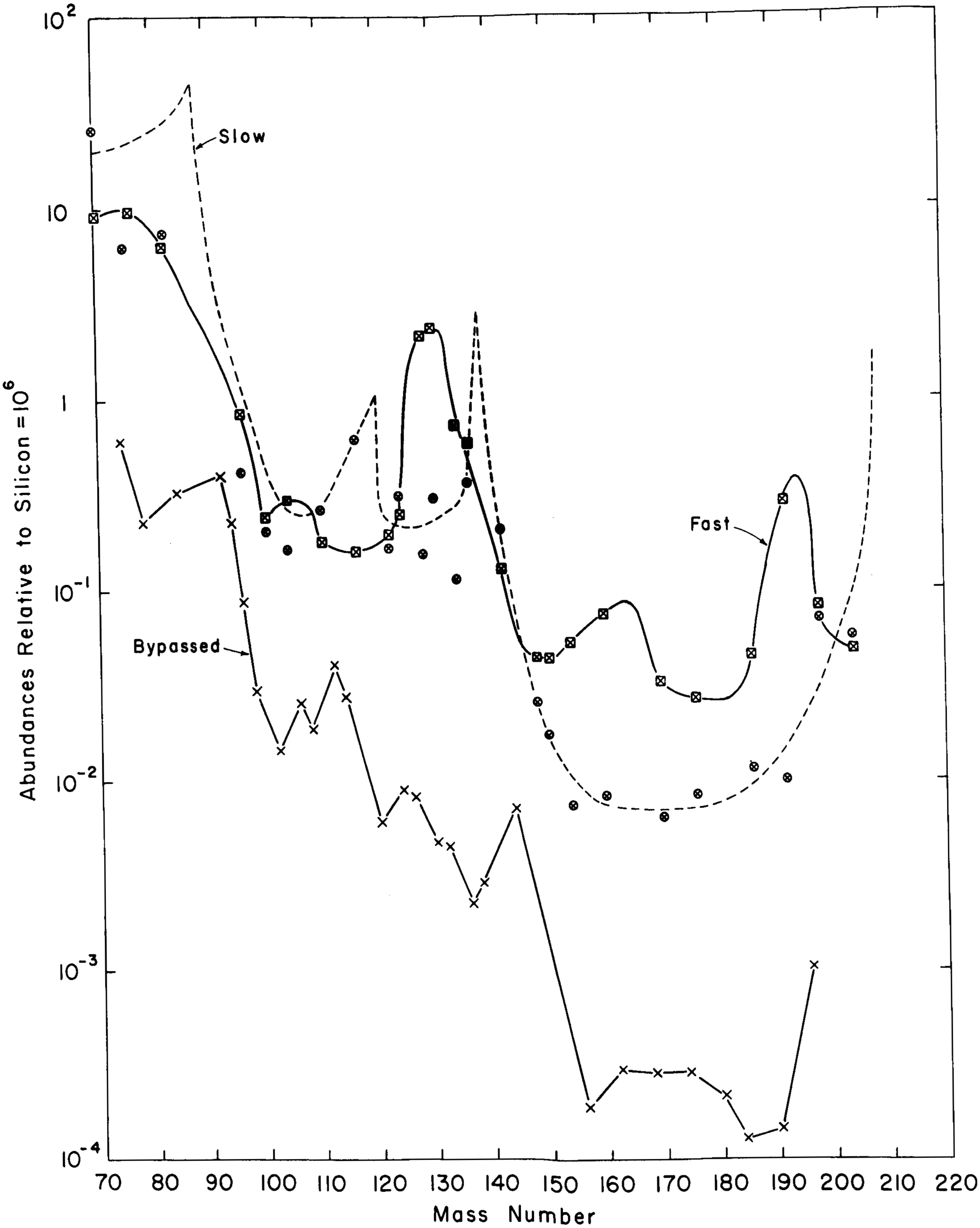

Slow
Fast
Bypassed
Abundances Relative to Silicon = 10^6
Mass Number
10^2
10
1
10^{-1}
10^{-2}
10^{-3}
10^{-4}
70 80 90 100 110 120 130 140 150 160 170 180 190 200 210 220